Microstructural Changes in As-Cast M2 Grade High Speed Steel during Hot Forging

M.R. GHOMASHCHI and C.M. SELLARS

High speed steels have a complex carbide pattern in the as-cast state which has to be modified to achieve the desired properties of adequate toughness, hot hardness, and wear resistance. The effects of hot forging and postdeformation annealing on carbide distribution and morphology in M2 grade high speed steel were studied, and it was shown that hot forging accelerates the spheroidization rate of M_6C carbide with little effect on coarsening. The mechanism responsible for such acceleration is dominated by mechanical disintegration of M_6C carbide plates, while diffusion-controlled spheroidization was not significant. For MC carbide particles, coarsening was the dominant mechanism, but it was not possible to ascertain whether diffusion had been unaffected by deformation or even increased by a factor that could be as high as 10,000 times. Annealing after deformation accelerated spheroidization which was attributed to the damaging of carbide plates during forging rather than an increase in diffusion rate, since the matrix was almost substructure-free in the annealed condition, *i.e.*, lack of short-circuiting paths for diffusion.

I. INTRODUCTION

HIGH speed steels, primarily used for the manufacture of cutting tools, have a complex carbide pattern in the as-cast state. The heavily segregated carbide zones should be modified to achieve uniform carbide distribution, and after appropriate heat treatment, the finished tool should have the following properties: (1) adequate strength; (2) strength retention at temperature; (3) adequate toughness; (4) resistance to thermal shock; and (5) resistance to wear.

In order to break down the carbide networks in high speed steels, the as-cast steel is initially hot forged at high temperatures, *e.g.*, 1100 °C to 1140 °C for the M2 grade, with the final forging pass carried out at temperatures not less than 900 °C. This is then followed by heat treatment, which for M2, consists of hardening at 1210 °C to 1230 °C and usually double tempering at 550 °C to 570 °C.

It is generally believed that high-temperature deformation of steel increases the rate of spheroidization and coarsening of carbides. The theories proposed to explain spheroidization are all based on enhanced diffusivity due to the following:

(1) formation of short-circuiting diffusion paths during deformation, *i.e.*, dislocations and/or subgrain boundaries;[1,2,3]
(2) generation of excess vacancies and formation of solute/vacancy complexes;[1,4–6] and
(3) geometric role played by substructures formed in one or both phases, which leads to enhanced diffusion rate and subsequent spheroidization.[7,8]

The theories proposed for enhanced coarsening rate due to deformation are all based on the original theories developed by Greenwood,[9] Lifshitz and Sloyosov,[10,11] and Wagner.[12] The increase in coarsening rate was attributed to enhanced diffusivity, as has already been mentioned for accelerated spheroidization,[13,14,16] although the geometric role of substructure is not clearly defined.

The present investigation is undertaken to study the effect of deformation on carbides in M2-grade high speed steel. This is the last article in a series of articles[15–18] on the effect of thermal and thermomechanical treatments on carbides in as-cast M2-grade high speed steel.

II. MATERIAL AND EXPERIMENTAL PROCEDURES

The material used in this study, M2 high speed steel, was prepared in the laboratory by air melting using ARMCO iron as the base material, and white cast iron, ferrotungsten, ferrovanadium, pure chromium, and pure molybdenum were added to achieve the chemical composition of (weight percent) C0.86, W6.85, Mo5.3, Cr4.22, V1.96, Mn0.07, and Si0.25 (fully killed). The trace elements of Nb, Ti, Co, and Au were <0.02 pct.

*ARMCO is a trademark of Armco, Inc., Middletown, OH.

Rectangular specimens of 25 × 25 × 35 mm were slit, ground, and upset forged with a 50 ton hydraulic press. All specimens were reheated for 2 hours at 1200 °C and 1150 °C before forging. In order to mitigate the quenching effect of the press anvils, all specimens were sandwiched between two superalloy platens which were heated to the forging temperatures. The temperature changes were monitored during deformation with K-type thermocouples installed either within the center of the specimen or the top superalloy platen.

M.R. GHOMASHCHI, Lecturer in Materials Processing, is with the Metallurgy Department, University of South Australia, Levels Campus, The Levels, S.A. 5095, Australia. C.M. SELLARS, POSCO Professor of Iron and Steel Technology and Head, is with the Department of Engineering Materials, University of Sheffield, Sheffield, United Kingdom.

Manuscript submitted September 1, 1992.

All tests were carried out unlubricated, *i.e.*, in the dry condition, and the experimental procedures are given in Table I. All specimens were sectioned longitudinally and polished conventionally on emery papers and diamond pastes of 6, 1, and 0.25 μm. Full details of etching procedures and analytical facilities used for microstructural examinations have been previously given.[15] The method used to obtain stress/strain distribution within the upset forged specimens is presented elsewhere.[19]

In order to measure the percentage of spheroidized M_6C and the total amount of MC and M_6C carbides, systematic point counting was selected as the method of estimation. The measurements were carried out on parallel lines on the plane of polish utilizing an optical microscope with a traveling stage connected to a digital counter which moved the stage in 0.05-mm increments. A total number of 1200 points were counted for each specimen to reduce the statistical error to less than 1 pct.

For size distribution analysis of MC and M_6C carbides, a semiautomatic Carl Zeiss particle size analyzer was used in conjunction with optical micrographs taken from specimens etched electrolytically in chromic acid solution. The size evaluation is based on the equivalent circle area diameter (ECAD), that is, the diameter of a circle having the same area as the object to be measured, *i.e.*, an MC or M_6C carbide. A total number of 250 particles were measured for each specimen, and the arithmetic mean particle size $\bar{d}$ was calculated.

III. RESULTS

A. *Microstructure*

As mentioned by the present author[15,18] and recently by others,[20,21] the as-cast structure contains coarse eutectic carbides of MC, M_2C, and M_6C which segregate at the prior austenite grain boundaries during solidification. As shown in Figure 1, the as-cast structure also consists of the central large and small carbides.[15] The M_2C carbide is unstable at the reheating temperatures of 1150 °C or 1200 °C and transforms fully to MC and M_6C in less than 1 hour. This means that the effect of deformation could only be studied on M_6C and MC carbides, since as mentioned (Table 1), all specimens were reheated for 2 hours at 1150 °C or 1200 °C before forging. The actual forging temperature, however, was about 1000 °C, as can be ascertained from the time-temperature graph in Figure 2, which shows temperature variations for the last 15 minutes of the reheating operation and subsequent forging.

As expected, the strain distribution during upset forging is not uniform (Figure 3), and therefore, careful analysis of a single specimen should be adequate to estimate the critical strain required to break down the reticular character of the eutectic carbide network. The resultant carbide bands (Figure 3(c)) consist of disintegrated M_6C particles formed by mechanical fragmentation and/or the formation of edgewise channels within the M_6C plates. The scanning electron micrographs in

Table I. Procedures of Deformation*

Specimen	Reheating before Deformation (h)	Reduction (Pct)	Load (Ton)	Procedures after Deformation	Temperature (°C)	Cast Structure
F17	2	39.6	12.5	quenched	1200	sand
F18	2	37.5	12.5	1 h reheat + quenched	1200	sand
F19	2	34	12.5	quenched + 1 h reheat + quenched	1200	sand
F20	2	32	14.75	quenched	1150	sand
F21	2	30.4	13	1 h reheat + quenched	1150	sand
F22	2	29.3	14.25	quenched + 1 h reheat + quenched	1150	sand
F23	2	41.87	10.25	2 h reheat + quenched	1200	sand
F24	2	39.6	10.25	10 h reheat + quenched	1200	sand
F25	2	38	12.5	2 h reheat + quenched	1150	sand
F26	2	38	17	10 h reheat + quenched	1150	sand
F27	2	55	14.25	quenched	1200	sand
F28	2	54	12	1 h reheat + quenched	1200	sand
F29	2	54	12.5	2 h reheat + quenched	1200	sand
F30	2	59.6	18.75	10 h reheat + quenched	1200	sand
F31	2	53	17.25	10 h reheat + quenched	1150	sand
F32	2	54	24	2 h reheat + quenched	1150	sand
F33	2	51	16.5	1 h reheat + quenched	1150	sand
F34	2	50	15.5	quenched	1150	sand
F35	10 + quenched	65.5	20	quenched	1200	sand
F36	10 + quenched	64.3	33.75	quenched	1200	chill
F37	10 + quenched	62	22.5	1 h reheat + quenched	1200	sand
F38	10 + quenched	63.6	23.5	1 h reheat + quenched	1200	chill
F39	10 + quenched	70	26.25	2 h reheat + quenched	1200	sand
F40	10 + quenched	68.5	31.25	2 h reheat + quenched	1200	chill
F42	10 + quenched	62	26.25	quenched	1200	sand
F46	10 + quenched	64.1	22.75	quenched	1200	sand

*All quenching was carried out in water. F35 through F46 were reheated for 15 minutes before forging. All specimens were sandwiched between two superalloy platens and heated to the forging temperatures.

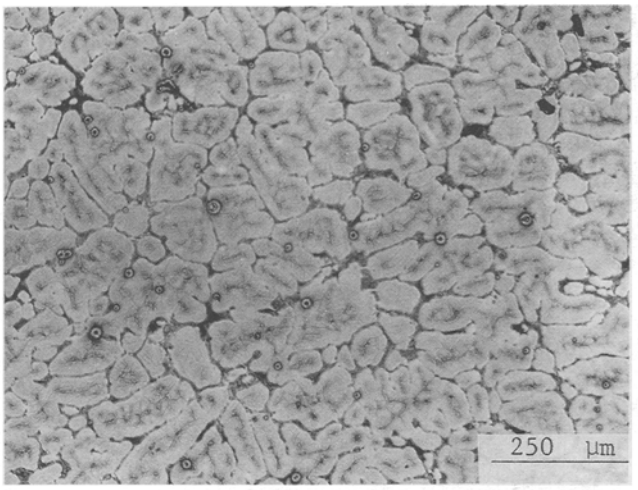

(*a*)

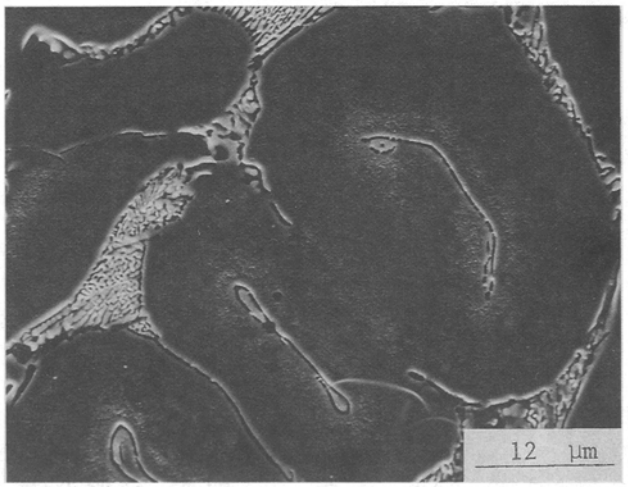

(*b*)

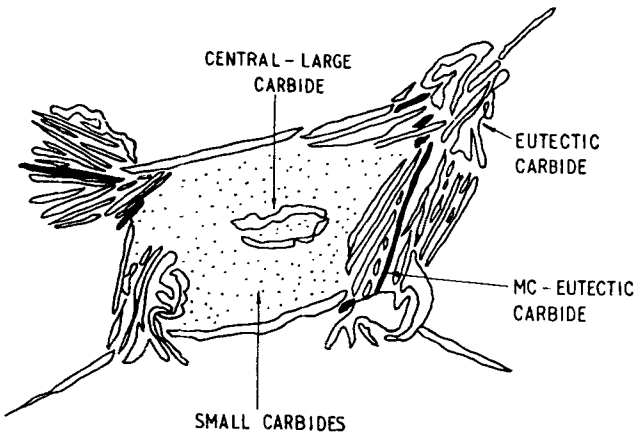

(*c*)

Fig. 1 — As-cast structures of M2-grade high speed steel: (*a*) optical micrograph (etchant: nital + K MnO_4); (*b*) SEM micrograph to show different carbides (etchant: K MnO_4); and (*c*) schematic diagram to show different carbides.

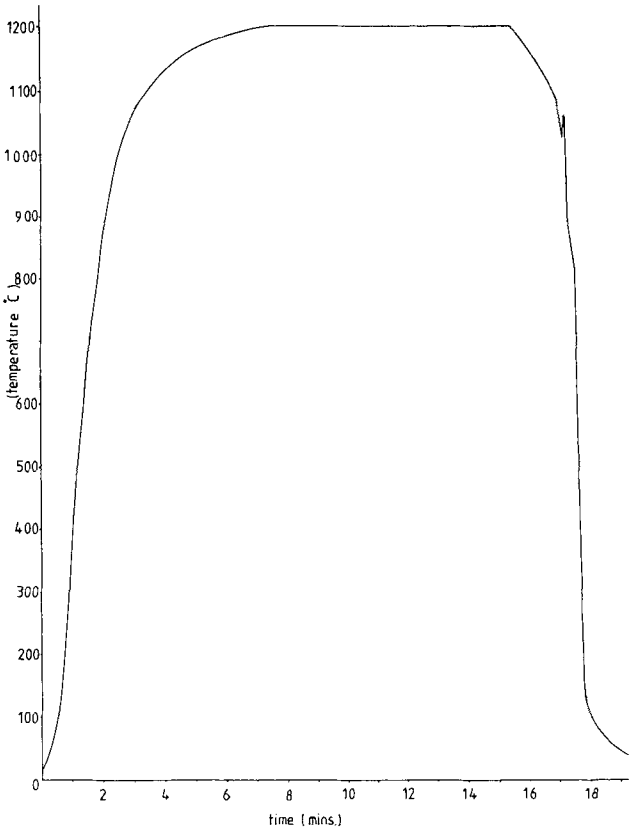

Fig. 2 — Typical temperature variations at the center of rectangular specimens during reheating, forging, and quenching operations. (The final stages of reheating and the forging/quenching operations are as shown here.)

Figure 4 clearly show both mechanisms. The formation of diffusion-controlled edgewise channels appears to be the minor mechanism. The morphology of MC eutectic carbide remains mainly unchanged, although its mean size is slightly greater than that of similar time and temperature during static annealing.[16] In addition, some spheroidization of the M_6C central large carbides has taken place along with a considerable general dissolution of small carbides. Furthermore, a few intragranular grown carbides have been detected.[15] The matrix, on the other hand, shows some degree of grain growth especially in regions where the strain is maximum or the density of small carbides is low. The optical micrograph in Figure 5 demonstrates the changes which have occurred in the as-deformed specimens.

During postdeformation annealing, the sharp tips of the mechanically fragmented eutectic carbides disappeared and further spheroidization of M_6C plates was observed (Figure 6). In addition, the size of carbide particles is slightly greater than that of the statically annealed specimens of similar time and temperature.[16] The matrix has an equiaxed grain structure with some degree of grain growth especially near the central region of the specimen where strain is maximum.

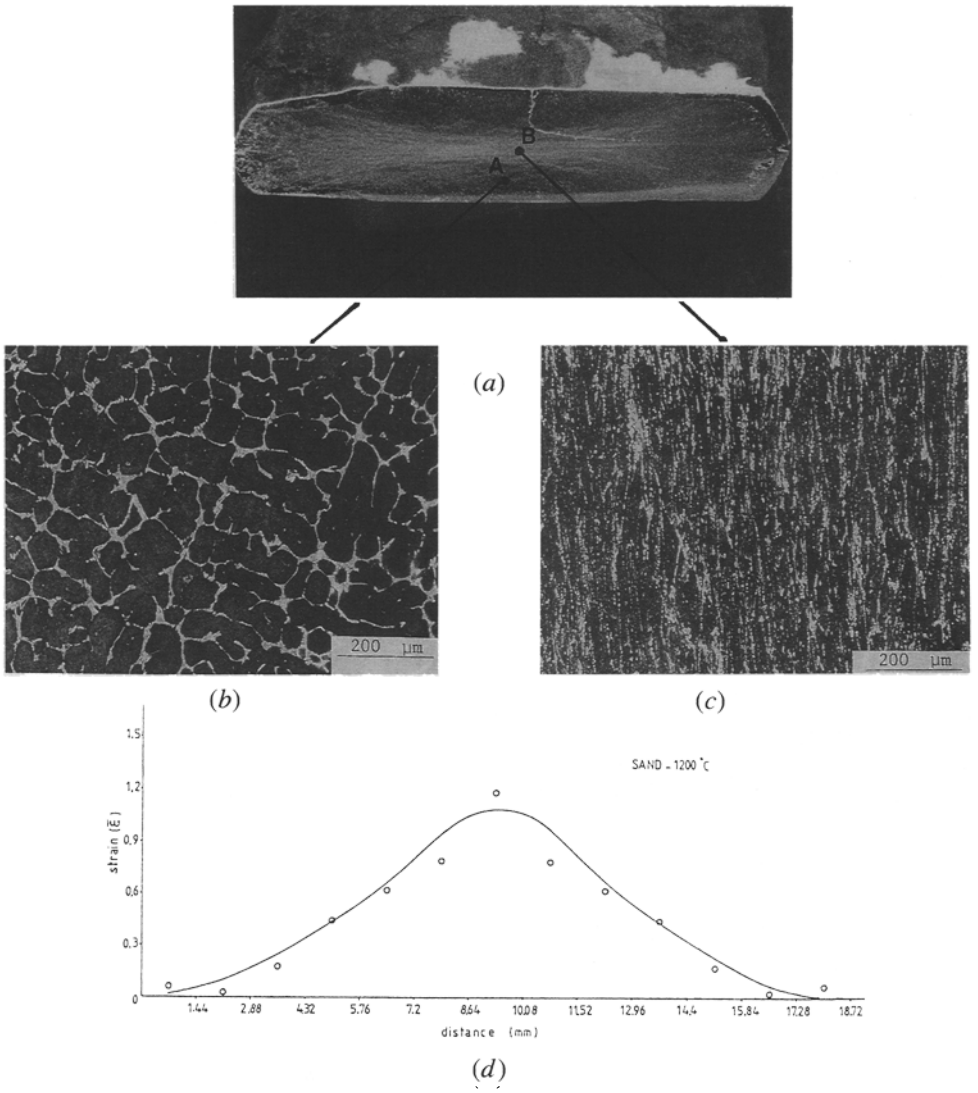

Fig. 3—(*a*) as-forged to show strain distribution; (*b*) and (*c*) optical micrographs taken from points *A* and *B* in (a); and (*d*) strain distribution.

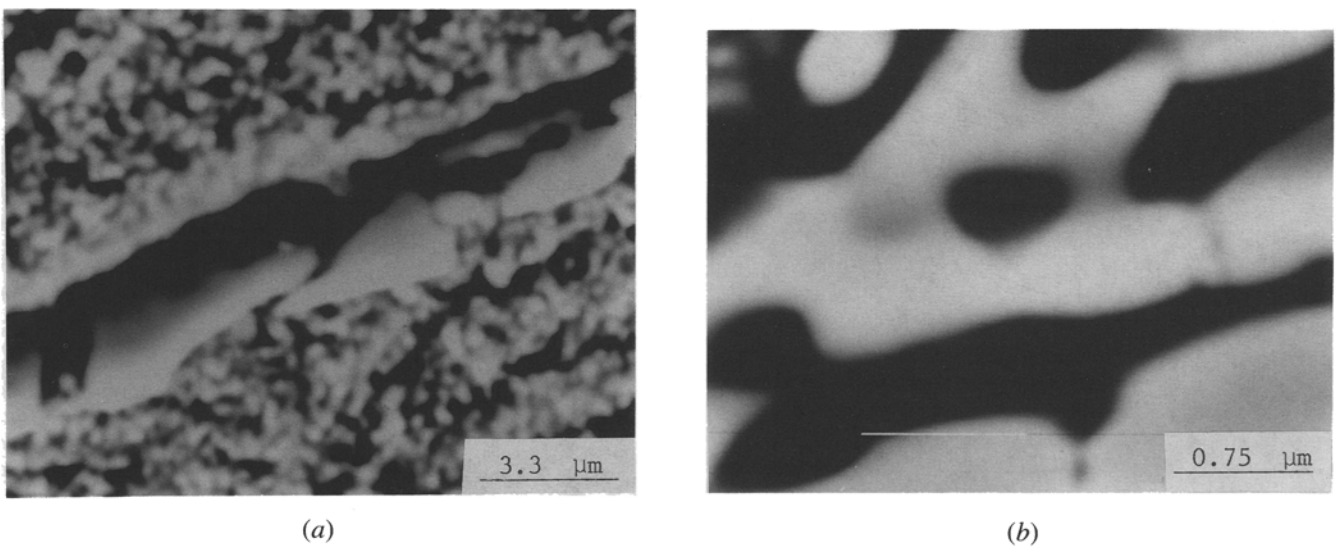

Fig. 4—SEM micrographs taken from the as-deformed specimen to show carbide disintegration during forging: (*a*) mechanical fragmentation and (*b*) spheroidization by edgewise channel formation.

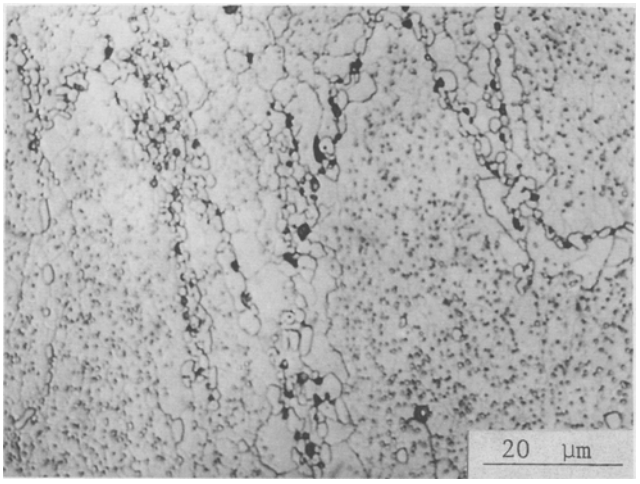

Fig. 5—Optical micrograph taken from the central regions of the as-forged F17 specimen to show general carbide dissolution and matrix structure.

B. *Quantitative Metallography*

1. *Volume fraction*

The volume fraction of the eutectic carbides (MC and M_6C) was measured for the as-deformed and post-deformation annealed specimens. As illustrated in Table II, the volume fraction of the eutectic carbides is almost constant and is slightly lower than that of the statically annealed specimens of similar time and temperature.[16] The volume fraction of the intragranular grown carbides is marginally greater.[16]

In order to study the effect of deformation on the morphology of carbides, the percentage of spheroidized eutectic carbides was measured. Particles with aspect ratio (length/width) ≤ 5 were counted as spheroids. This measurement was carried out on M_6C carbide only, since as mentioned in Section III–A, the majority of MC carbide particles have aspect ratios ≤ 5, *i.e.*, spheroids. The results are tabulated in Table III and plotted in Figure 7. As is evident, deformation is quite effective on spheroidization of the M_6C carbide plates and, furthermore, the percentage spheroidization is a function of applied strain. In addition, the application of postdeformation annealing has caused further spheroidization of M_6C carbide. The reheating temperature before or after deformation could also influence the degree of spheroidization.

2. *Size distribution*

a. *MC*

As mentioned in Sections III–A and III–B–1, the majority of MC carbide particles have spheroidal shape and, therefore, deformation is expected to influence the size rather than the morphology of this carbide. As illustrated in Table IV and plotted in Figure 8, the mean

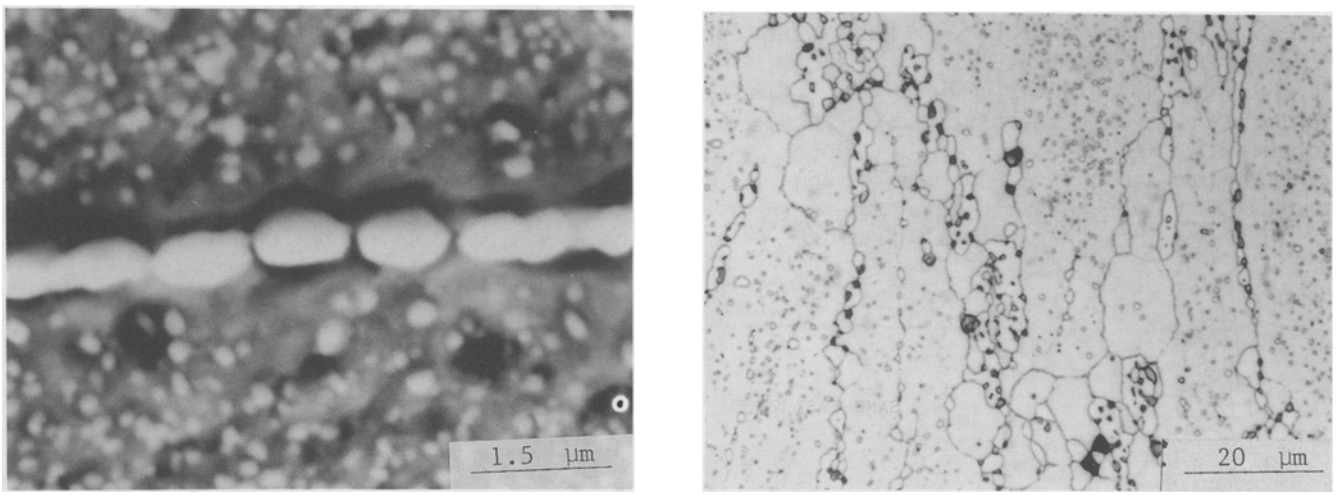

(*a*) (*b*)

Fig. 6—(*a*) SEM micrograph taken from F26 specimen to show the effect of postdeformation annealing on the mechanically fragmented eutectic carbide. (*b*) Optical micrograph taken from F23 to show the effect of postdeformation annealing on carbides and matrix structure.

Table II. Volume Fraction of Eutectic MC and M_6C Carbides and Intragranular Grown Carbides at Both 1150 °C and 1200 °C (Sand Cast)

Specimen	H53	F17	F18	F19	H64	F20	F21	F22
MC pct	1.7 ± 0.3	1.5 ± 0.3	1.6 ± 0.3	1.5 ± 0.3	1.5 ± 0.3	1.6 ± 0.3	1.6 ± 0.3	1.4 ± 0.3
M_6C pct	9.5 ± 0.7	8.7 ± 0.6	10.1 ± 0.6	10.6 ± 0.7	10 ± 0.7	9 ± 0.6	9 ± 0.6	8.5 ± 0.6
Intergranular carbide pct	0.4 ± 0.2	0.54 ± 0.2	0.78 ± 0.3	0.78 ± 0.3	0	0.61 ± 0.3	0.53 ± 0.2	0.50 ± 0.2

*H53: statically annealed—2 h at 1200 °C + water quenched.
H64: statically annealed—2 h at 1150 °C + water quenched.

Table III. Spheroidization Percentages at Various Locations for Sand-Cast Structure

Specimen	Local Strain (ε)	Spheroidization (pct)
(a) 1200 °C		
	0.375	81.7 ± 4.3
F17	1.230	90 ± 3.9
	0.240	92.5 ± 3.2
F18	1.200	98.5 ± 1.4
	0.435	98.2 ± 1.8
F23	0.885	100
	0.405	89.4 ± 3.8
F27	1.500	98.6 ± 1.4
	0.375	92.5 ± 3.2
F28	1.485	100
	0.510	97.1 ± 2.0
F29	1.500	100
(b) 1150 °C		
	0.270	56.3 ± 7.2
F20	1.050	80.4 ± 5.8
	0.330	62.9 ± 8.2
F21	0.950	74.5 ± 6.4
	0.105	90.2 ± 3.8
F25	1.140	97 ± 2.1
	0.420	80.3 ± 5.1
F34	1.260	94 ± 3.4
	0.420	91.7 ± 3.6
F33	1.335	98.4 ± 1.6
	0.150	100
F32	1.320	100

size, $\bar{d}$, has increased with strain and temperature. Subsequent postdeformation annealing has rendered a similar trend, although the slope is slightly greater than that for the as-deformed specimens (Figure 9). The size distribution histograms in Figure 10 clearly demonstrate the effect of strain and temperature on the coarsening of MC carbides; *i.e.*, the mean particle size increases, moves to the right, with increasing strain or temperature.

b. M_6C

The M_6C carbide, unlike the MC, is very sensitive to deformation; *i.e.*, both the size and morphology of M_6C carbide vary with deformation. The average size and strain are given in Table IV and plotted in Figures 8 and 9 for the as-deformed and postdeformation annealed specimens. For the as-deformed specimens, the trend is as expected, where particle size decreases with increasing strain while annealing increases the average M_6C size. The size distribution histograms (Figure 10) support such conclusions.

IV. DISCUSSION

The barrel shape of the cube specimens (Figure 3(a)) and the normal distribution of strain (Figure 3(d)) plus the presence of dead zones during upset forging[22] (Figure 3(b)) are all indicative of a nonuniform size distribution of carbides in one single forged specimen. Furthermore, cracking restricts the maximum percentage reduction achievable in one single pass. In order to reduce cracking as much as possible, deformation should be carried out fairly quickly to prevent temperature drop. However, cracking may be prevented by appropriate selection of strain rate and strain values along with multipass deformation.

A. *As Forged*

Since all specimens were preheated at least 2 hours before forging, the microstructural characteristics should be the same as discussed for the statically annealed specimens[15] of similar time and temperature, *i.e.*, small austenitic grain size, some degree of carbide dissolution, and complete transformation of M_2C to M_6C and MC carbides. The prime consequence of deformation is banding of the eutectic carbide colonies due to the greater deformability of the matrix in contrast to that of carbides. Apart from banding, there is an acceleration of

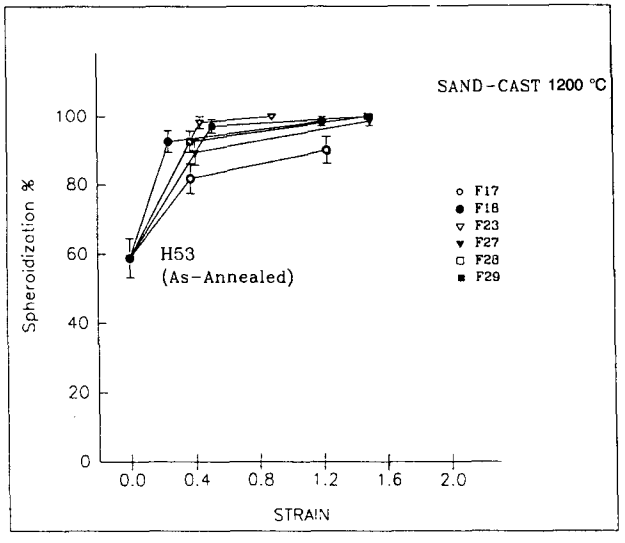

(*a*)

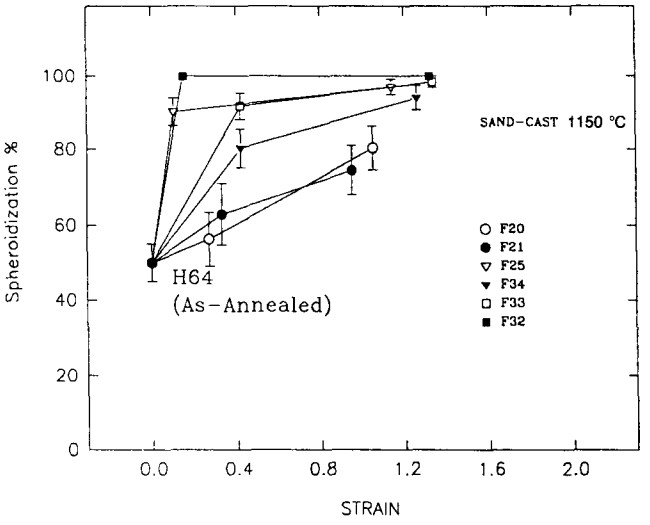

(*b*)

Fig. 7—Effect of hot forging and subsequent annealing operations on the percentage of spheroidized M_6C carbide: (*a*) 1200 °C and (*b*) 1150 °C.

Table IV. Mean size, $\bar{d}$, of MC and M_6C grain boundary carbides at Various Locations for Sand-Cast Structures Deformed at 1200 °C

Sample	$\bar{d}_{MC}$ (μm)	Standard Deviation	Standard Error	$\bar{d}_{M_6C}$ (μm)	Standard Deviation	Standard Error	Local Strain
F17	0.585	0.198	0.014	1.11	0.398	0.033	0.180
	0.575	0.189	0.014	1.05	0.334	0.024	1.11
	0.628	0.216	0.018	1.01	0.332	0.030	1.23
F18	0.540	0.184	0.015	1.15	0.360	0.030	0.210
	0.597	0.200	0.016	1.35	0.410	0.032	0.950
	0.578	0.227	0.018	1.25	0.357	0.025	1.13
F19	0.639	0.205	0.019	1.32	0.423	0.041	0.340
	0.672	0.238	0.017	1.29	0.373	0.031	0.870
	0.725	0.242	0.017	1.40	0.380	0.027	1.10
F23	0.512	0.150	0.012	1.20	0.404	0.039	0.450
	0.539	0.175	0.015	1.36	0.442	0.040	0.840
	0.551	0.178	0.012	1.32	0.444	0.038	1.155
F24	0.542	0.192	0.015	1.44	0.537	0.054	0.345
	0.515	0.159	0.012	1.36	0.455	0.033	0.900
	0.581	0.228	0.019	1.26	0.342	0.034	1.155
F27	0.457	0.129	0.008	1.07	0.378	0.027	0.278
	0.502	0.165	0.012	1.02	0.328	0.023	1.080
	0.557	0.194	0.016	1.07	0.340	0.024	1.478
F28	0.563	0.209	0.014	1.17	0.400	0.027	0.180
	0.637	0.250	0.023	1.29	0.450	0.033	0.995
	0.720	0.276	0.023	1.32	0.442	0.033	1.275
F29	0.590	0.215	0.018	1.27	0.411	0.032	0.315
	0.620	0.231	0.018	1.35	0.429	0.033	1.148
	0.701	0.309	0.031	1.44	0.478	0.040	1.500
F37	0.629	0.223	0.030	1.70	0.651	0.052	0.512
	0.943	0.503	0.072	2.15	0.867	0.080	1.200
	1.16	0.691	0.111	2.06	0.752	0.071	—
F39	0.911	0.412	0.040	1.81	0.668	0.060	0.720
	0.951	0.435	0.044	1.95	0.651	0.052	0.992
	1.08	0.483	0.054	2.12	0.718	0.066	—
F42	0.658	0.256	0.027	1.64	0.615	0.041	0.601
	0.718	0.289	0.028	1.92	0.629	0.044	1.045
	0.682	0.275	0.026	1.78	0.632	0.040	—
F46	0.739	0.274	0.027	1.93	0.723	0.062	0.645
	0.768	0.327	0.029	1.64	0.610	0.038	1.100
	0.727	0.297	0.027	1.72	0.587	0.036	—

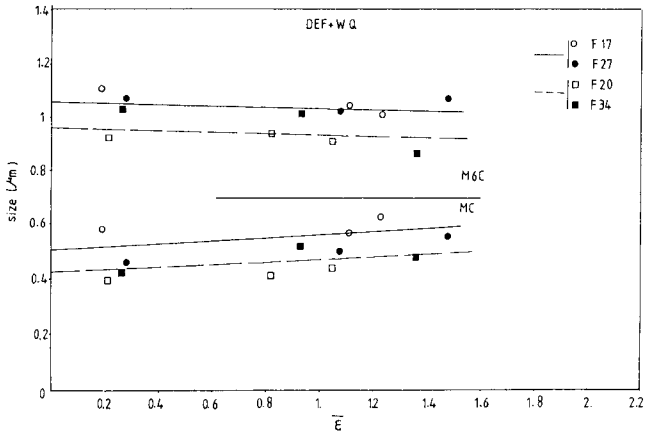

Fig. 8—Effect of strain on the mean size of grain boundary MC and M_6C carbides in the as-deformed specimens at 1200 °C (○, ●) and 1150 °C (□, ■).

spheroidization rate where the percentage of spheroidized carbide plates has risen considerably in comparison with the statically annealed specimens. For example, H53, which was heated 2 hours at 1200 °C, contained about 55 to 60 pct spheroidized M_6C compared with 80 to 90 pct in the deformed specimens, *i.e.*, F17 and F27. The same conclusion may be reached if the histograms of Figure 10 are studied carefully. It is evident that the frequency of finer particles has increased with strain at the middle and central regions.

The matrix structure has changed during forging where elongated and equiaxed grains have been observed mainly at the central regions (Figure 5). As reported previously,[15] the reheated steel consists of very fine and stable austenite grains. However, the size of grains in the deformed specimens is almost one order of magnitude larger than that of the statically annealed specimens. Furthermore, this confirms the fact that they

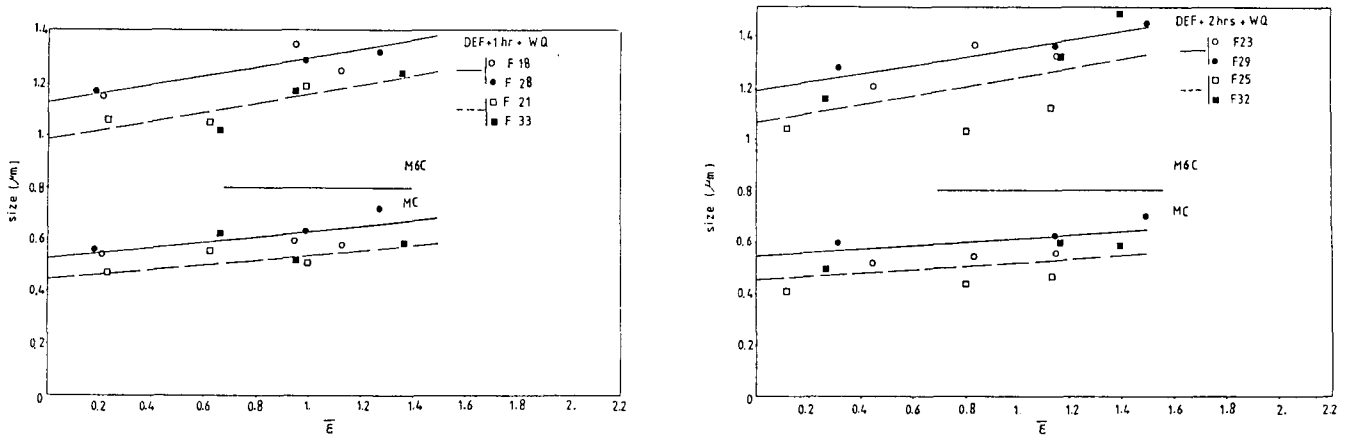

(a) (b)

Fig. 9—Effect of strain on the mean size of grain boundary MC and M_6C carbides in specimens annealed after deformation at 1200 °C (○, ●) and 1150 °C (□, ■). Annealing times are (*a*) 1 h and (*b*) 2 h.

are true grains not subgrains. The larger grain size confirms the increase in diffusion rate needed for grain growth and the fact that the grains are mainly detectable within the central region; *i.e.*, larger strains confirm the effectiveness of deformation on diffusion. The equiaxed grains, however, should have formed at the end of deformation and just before quenching.

The majority of MC carbide particles had aspect ratios ≤5, *i.e.*, spheroids, and therefore were mainly subjected to coarsening, whereas the M_6C particles had undergone both spheroidization and coarsening. Previous works on spheroidization and coarsening of carbides, up to 700 °C reheating temperatures, revealed gross acceleration of both the processes due to an increased diffusion rate.[1,6]

Considering MC first, Figure 8 reveals a slight size increase during forging. Unfortunately, there are no data available for acceleration of diffusion in austenite for the temperature range used in the present investigation. However, it is possible to obtain a guideline using Eq. [1] for α-iron given by Hirano *et al.*[23] with the following assumptions:

(1) it is applicable at high temperatures, 1150 °C to 1200 °C; and
(2) it may be applied to γ-iron,

$$\left(\frac{D_s}{D_u} - 1\right) = \frac{N_x}{N_v} = \beta\dot{\varepsilon} \qquad [1]$$

where D_s and D_u are self-diffusivities of strained and unstrained specimens, N_v and N_x are the thermal equilibrium vacancy concentration and excess vacancy generated by plastic deformation, respectively, β is strain rate factor, $\beta = 3 \times 10^{-3} \exp 19{,}700/T$, and $\dot{\varepsilon}$ is the strain rate (s^{-1}). The value of β was calculated at 1150 °C and 1200 °C. The D_s/D_u at 1200 °C is then calculated as 991. Therefore, the diffusion rate may have been accelerated by a factor of 1000 times as a result of plastic deformation. It was shown[16] that bulk diffusion of vanadium with a rate constant value of $K = 2.26 \times 10^{-6}$ $\mu m^3/s$ is the mechanism responsible for coarsening of MC particles during static annealing. The actual size of the MC particle just before deformation, after 2 hours at 1200 °C, is about 0.5 μm (Figure 8). Therefore, during the time, about 2.5 seconds, taken to upset forge cubic specimens, the size of MC carbide would be predicted to increase to only $d = 0.57$ μm, which is within the range of experimental scatter. Therefore, within the experimental scatter, it is not possible to distinguish whether diffusion has been unaffected by deformation or increased by a factor that could be as high as 10,000 times.

In contrast to MC, the M_6C carbide shows a drop in mean size with strain which is quite predictable due to spheroidization. Although spheroidization of M_6C carbide is evident in Figures 3 through 5, the quantitative results in Figures 7 and 10 confirm the dominance of such a mechanism during deformation. Comparison of the results in Figure 7 and those obtained for undeformed specimens[16] reveals that on a time basis, spheroidization is accelerated by a factor of 1.5×10^5 times. This is at least one order of magnitude greater than the maximum possible acceleration of diffusion rate. This is in confirmation of the qualitative analysis of the microstructure where mechanical fragmentation is the dominant mechanism of spheroidization. Furthermore, if rapid spheroidization is due to strain-enhanced diffusion rate, then the rate of coarsening which is solely diffusion dependent should have also increased. In other words, the size of M_6C particles should increase with strain. Figure 11, which shows the size changes of the top 25 pct largest M_6C particles against strain, does not support such hypothesis.

B. *Annealing*

Annealing of the deformed specimens modifies the microstructure in two ways: (1) recrystallization of matrix; and (2) coarsening and further spheroidization of carbides.

The substructure-free grains in Figure 6(b) are due to recrystallization during annealing. In addition, some degree of grain growth has been detected, particularly at regions with low densities of small carbides. Therefore,

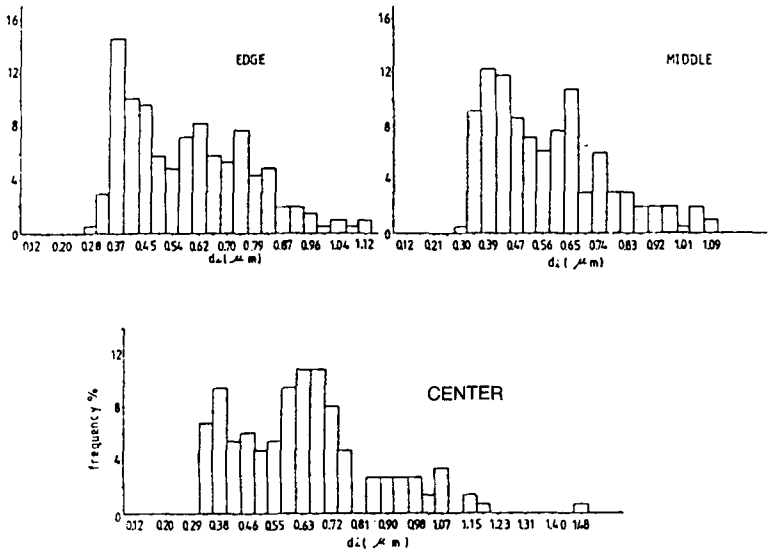

(*a*) **As-deformed-MC**

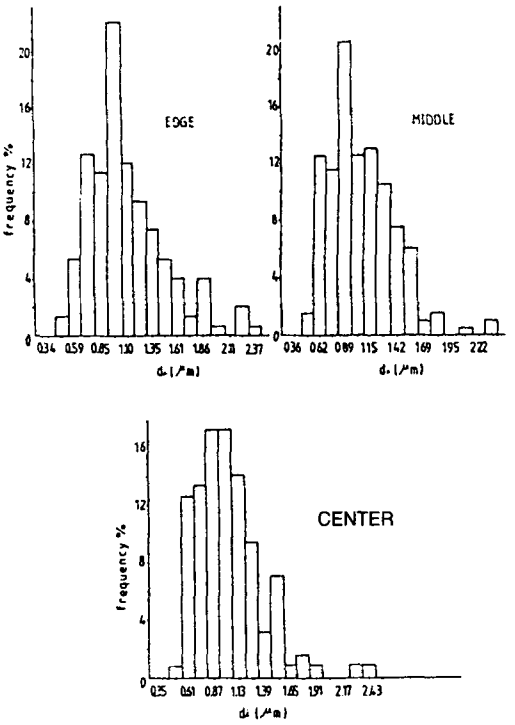

(*c*) **As-deformed-M_6C**

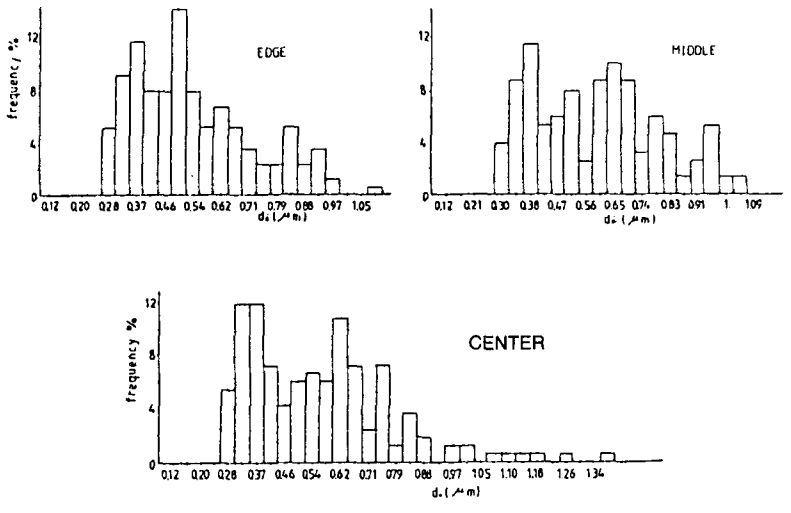

(*b*) **Deformed and annealed - MC**

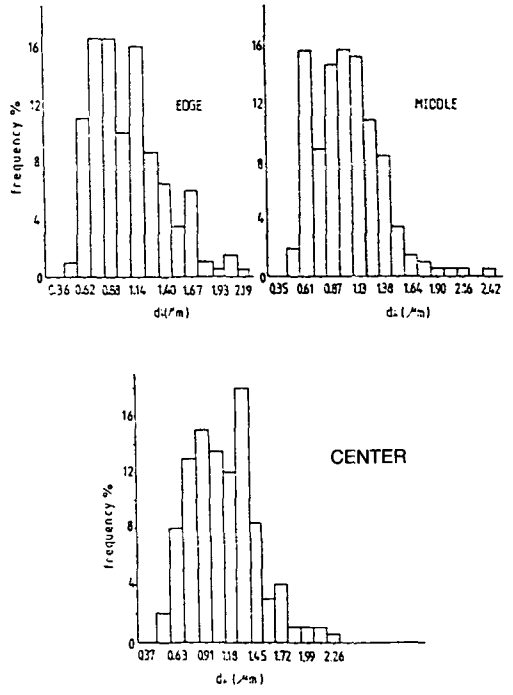

(*d*) **Deformed and annealed M_6C**

Fig. 10—Size distribution histograms for grain boundary carbides in as-deformed and postdeformation annealed specimens: (*a*) as-deformed MC; (*b*) deformed and annealed MC; (*c*) as-deformed M_6C; and (*d*) deformed and annealed M_6C.

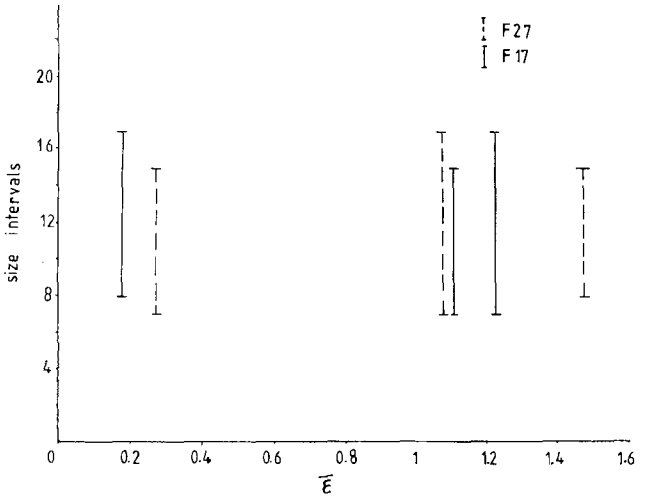

Fig. 11—The effect of strain on the size of the top 25 pct largest M_6C particles in F17 and F27 specimens. Size intervals refer to the interval limits of the Carl Zeiss particle size analyzer used in this investigation and vary between 1 to 48, *i.e.*, 1.4 to 27.7 mm. The values above represent the effect of strain on the size changes only, and thus, the actual values are not important.

the small carbides have been effective in pinning the boundaries, which is why a very fine grain structure has formed in both annealed and deformed specimens.

Furthermore, the sharp-tipped fragmented carbides become smooth, while the remaining M_6C plates undergo further spheroidization. The slightly increased rate of spheroidization may be attributed to the damage inflicted on carbides during deformation rather than the matrix, since the matrix contains almost substructure-free grains, *i.e.*, absence of short-circuiting paths. The almost fully spheroidized MC particles have not shown a major increase in coarsening rate, which could be attributed to their uniform size and obviously to the matrix structure.

V. CONCLUSIONS

The following conclusions may be drawn from the present study.

1. Hot forging accelerates the spheroidization rate of M_6C carbides, while it has little apparent effect on coarsening.
2. The mechanism of accelerated spheroidization of M_6C carbides is dominated by mechanical fragmentation of plates; diffusion phenomena play almost no role in this process, although MC carbides show a very small size increase during deformation which is within the experimental scatter. Therefore, it is not possible to ascertain whether diffusion has been unaffected by deformation or even increased by a factor that could be as high as 10,000 times.
3. Small substructure-free grains form during hot forging. Grain growth occurs during subsequent annealing.
4. The mechanism of spheroidization of M_6C plates is slightly accelerated during annealing after deformation, while the coarsening process is more or less the same as the heat-treated specimens. The minor acceleration of spheroidization might be attributed to the damaging of carbide plates during forging, since the matrix is almost substructure free, *i.e.*, absence of short-circuiting paths for diffusion.

REFERENCES

1. J.L. Robbins, O.C. Sheppard, and O.D. Sherby: *J. Iron Steel Inst.*, 1964, vol. 202, pp. 804-07.
2. E.A. Chojnowski and W.J. Tegart: McG.: *Met. Sci. J.*, 1968, vol. 2, pp. 14-18.
3. J.J. Jonas, C.M. Sellars, and W.J. Tegart: McG.: *Metall. Rev.*, 1969, vol. 14, pp. 1-24.
4. A.L. Ruoff and R.N. Balluffi: *J. Appl. Phys.*, 1963, vol. 34, pp. 2862-72.
5. M.J. Harrigan and O.D. Sherby: *Mater. Sci. Eng.*, 1971, vol. 7, pp. 177-89.
6. S. Chattopadhyay and C.M. Sellars: *Acta. Metall.*, 1982, vol. 30, pp. 157-70.
7. H. Paqueton and A. Pineau: *J. Iron Steel Inst.*, 1971, vol. 209, pp. 991-98.
8. D.F. Lupton and D.H. Warrington: *Met. Sci. J.*, 1972, vol. 6, pp. 200-04.
9. G.W. Greenwood: *Acta. Metall.*, 1956, vol. 4, pp. 243-48.
10. I.M. Lifshitz and V.V. Slyosov: *Zh. Eksp. Teor. Fiz.*, 1958, vol. 35 (2), p. 8.
11. I.M. Lifshitz and V.V. Slyosov: *J. Phys. Chem. Solids*, 1961, vol. 19 (1–2), pp. 35-50.
12. C. Wagner: *Z. Electrochem.*, 1961, vol. 65, p. 581.
13. W.E. Stumpf: Ph.D. Thesis, University of Sheffield, Sheffield, United Kingdom, 1968.
14. T. Mukherjee: Ph.D. Thesis, University of Sheffield, Sheffield, United Kingdom, 1969.
15. M.R. Ghomashchi and C.M. Sellars: *Met. Sci.*, 1984, vol. 18, pp. 44-48.
16. M.R. Ghomashchi and C.M. Sellars: University of South Australia, The Levels, unpublished research, 1993.
17. M.R. Ghomashchi: *Z. Metallkunde*, 1985, Band 76, Heft 10, pp. 701-03.
18. M.R. Ghomashchi: *Metall. Trans. A*, 1985, vol. 16A, pp. 2341-42.
19. M.R. Ghomashchi: *J. Strain Analysis*, 1984, vol. 19 (1), p. 71.
20. S. Karagöz, I. Liem, E. Bischoff, and H.F. Fischmeister: *Metall. Trans. A*, 1989, vol. 20A, pp. 2695-2701.
21. H.F. Fischmeister, R. Riedl, and S. Karagöz: *Metall. Trans. A*, 1989, vol. 20A, pp. 2133-48.
22. G.E. Dieter: *Mechanical Metallurgy*, 1976, McGraw-Hill, New York, NY.
23. K.I. Hirano, M. Cohen, B.L. Averbach, and N. Ujiiye: *Trans. AIME*, 1963, vol. 227, pp. 950-57.